27P

NASA Technical Memorandum 87301

3749

In-Flight Measurements of Wing Ice Shapes and Wing Section Drag Increases Caused by Natural Icing Conditions

Kevin Mikkelsen, Nikola Juhasz, Richard Ranaudo,
Robert McKnight, Robert Freedman, and John Greissing
Lewis Research Center
Cleveland, Ohio

April 1986

NASA

IN-FLIGHT MEASUREMENTS OF WING ICE SHAPES AND WING SECTION DRAG INCREASES CAUSED BY NATURAL ICING CONDITIONS.

Kevin Mikkelsen, Nikola Juhasz, Richard Ranaudo,
Robert McKnight, Robert Freedman, and John Greissing
National Aeronautics and Space Administration
Lewis Research Center
Cleveland, Ohio 44135

SUMMARY

Aircraft icing flight research was performed in natural icing conditions with a twin engine commuter type STOL aircraft. In-flight measurements were made of the icing cloud environment, the shape of the ice accretion on the wing, and the corresponding increase in the wing section drag. Results are presented for three icing encounters. On one flight, the wing section drag coefficient increased 35 percent over the uniced baseline for cruise conditions while a 43 percent increase was observed at an aircraft angle of attack of 6.2°.

NOMENCLATURE

C_d	wing section drag coefficient
C_l	wing section lift coefficient
c	wing cord, 1.98 m, 6.5 ft
KIAS	indicated airspeed, knots
KTAS	true airspeed, knots
LWC	cloud liquid water content, g/m^3
M	Mach number (calculated using aircraft true airspeed)
MVD	cloud median volume diameter droplet size, μm
OAT	static air temperature, °C
Re	Reynolds number (calculated using aircraft true airspeed and wing chord length)
α	aircraft angle of attack (referenced to waterline), deg

INTRODUCTION

The NASA Lewis Research Center's aircraft icing flight test program supports several program elements. One element of the program is to develop a flight test data base consisting of icing cloud parameter measurements, ice shapes, and aerodynamic measurements. The data base will be used to validate

the simulated icing produced in the NASA Lewis Icing Research Tunnel and to validate predictive computer codes. This paper presents in-flight measurements of the icing cloud parameters, the ice shapes on the wing, and the corresponding increases in wing section drag caused by ice for three natural icing encounters.

In-flight wing section drag measurements have been performed before for airfoils without ice. (refs. 1 and 2). The experiment consists of measuring both total and static pressures across the wake. The pressures are then related to the wing section drag coefficient using the Jones equation (ref. 1). While this flight experiment has been performed many times for airfoils without ice, no reference was found of it ever being done for airfoils with natural ice accretions on them. The presence of ice accretions on an airfoil can significantly increase drag and decrease lift. Many airfoil icing experiments have been performed in wind tunnels (refs. 3 and 4). A major icing wind tunnel facility is the NASA Lewis Icing Research Tunnel (IRT). The IRT can produce simulated icing conditions through the use of water spray bars and refrigerated air flow. Because small differences in icing parameters can produce large differences in ice shapes and hence large differences in the aerodynamic effects of ice (primarily at the warmer temperatures (see refs. 4 and 5)) simulation techniques should duplicate natural conditions as accurately as possible. Therefore a goal of current research is to compare wind tunnel simulated icing conditions to natural icing conditions observed in flight. In detail, it is desired to compare (1) the icing cloud parameters such as cloud liquid water content and water droplet sizes (2) the wing ice shapes resulting from the conditions and (3) the change in the wing section drag coefficient.

To accomplish this task and others the NASA Lewis Research Center is operating an icing research aircraft and using it to fly into known icing conditions. Work with this aircraft has resulted in three other reports to date (refs. 6 to 8). These reports have dealt primarily with icing instrumentation and overall aircraft performance loss due to ice. The experiment discussed in this report was conducted with the icing research aircraft during the late winter and spring of 1985 and was flown in the Cleveland, Ohio area.

In addition to the goal of improving simulated icing in the IRT, another goal is to use the flight test data to compare with computer predicted results. Several computer programs have been developed by NASA to predict droplet trajectories, ice accretions, and aerodynamic effects due to icing (ref. 9). While the goals are to make the comparisons described above, this paper presents only the flight test measurements of icing conditions, ice shapes, and drag increases.

THE AIRCRAFT

The icing research aircraft is a twin engine commuter type STOL aircraft, a DeHavilland DHC-6 Twin Otter. Maximum gross weight is 4990 kg (11 000 lb). Normal cruise airspeed is about 259 km/hr (140 KTAS) between the altitudes of 1829 m (6000 ft) and 3048 m (10 000 ft). Among the various ice protection systems on the aircraft are pneumatic boots on the wings outboard of the engine nacelles. The wing section itself has a NACA 6A series meanline and a modified NACA 0016 thickness distribution (ref. 10). The wing has no sweep back and no washout. The wing planform area is 39 m^2 (420 ft^2).

INSTRUMENTATION

Icing Instrumentation

Measurements were made of cloud liquid water content, median volume droplet diameter size, air temperature, and duration of the icing encounter. Icing environment data was recorded on a digital tape recorder. See figure 1 for icing instrument locations on the aircraft.

Instrumentation included:

LWC - Johnson and Williams heated wire probe produced by Cloud Technology.
MVD - Knollenberg Forward Scattering Spectrometer Probe (FSSP) produced by Particle Measuring Systems, Inc. (set for a range of 2 to 32 μm)
OAT - 102CA2W total temperature probe produced by Rosemount Inc.

It should be noted that the LWC and MVD icing cloud parameters are difficult to measure. Accuracy is difficult to determine and absolute calibrations are lacking. The instrumentation problem is very important, particularly for droplet sizes, but it is beyond the scope of this paper (see refs. 5 and 6). An important fact is that the above instruments were tested in the IRT and found to be repeatable. Therefore flight versus tunnel comparisons can be made.

Stereophotography System

A stereo camera system was developed for the icing research aircraft (fig. 2). The system produced stereo pair photo images of the wing's iced leading edge that enabled measurement of the ice surface through photogrammetric analysis with a minimum acceptable resolution of ±0.0762 cm (±0.03 in.). Two Hasselblad cameras were mounted in the nose of the aircraft behind optical glass viewports. The cameras' fields of view encompassed a common portion of the wing leading edge located ahead of the wake survey probe. To provide spatial references in the photo-images needed for photogrammetric analysis, an array of control points was painted on the wing leading edge section and the wing fence. To increase contrast and character of the ice surface in the image, a flash unit was mounted on the engine nacelle. The cameras and flash were activated from a switch at the copilot's station. The system is described more completely in reference 11.

Wing Wake Survey Probe

A wake survey probe was used to measure wing section drag coefficient. It was mounted on the wing behind the region where stereophotographs were taken. The probe had separate pitot and static probe tips located 1/4 chord aft of the wing trailing edge at about 69 percent of the semispan. The probe was driven by a motor inside the wing and could traverse an arc of 180° through the wing wake (fig. 3). Static and total pressures were measured by transducers located in the cabin. An analog x-y-y plotter in the cabin was used to record the pressure traces. During the icing flights, heaters in the probe kept the probe free of ice and a nitrogen purge system kept pressure lines clear of water.

Other Instrumentation

Altitude and airspeed were obtained from a pitot and static probe mounted on a noseboom. The tip of this pitot probe was 2.62 m (8.6 ft) in front of the aircraft nose. The position error associated with the noseboom static pressure source was calibrated using the trailing cone method. The difference between the noseboom and freestream static pressure was approximately 5.9 percent of the measured impact pressure with noseboom pressure greater than freestream. This percentage did not vary with angle of attack. The position error correction was factored into the calculation of the aircraft airspeed and altitude.

An angle of attack sensor was also added to the aircraft. This sensor was mounted on the side of the nose on the baggage compartment door. It was calibrated during steady level flight against an inclinometer on a floor rail. The angle of attack sensor was made by Specialities Inc. (Model SLZ2303). It should be noted that the engineering drawings for the aircraft indicate that the wing is at a positive 2.5° incidence to the waterline of the aircraft (the waterline is parallel to the floor line). The angle of attack sensor was referenced to the waterline of the aircraft. In addition to the 2.5° incidence of the wing, the local angle of attack of the wing at the section where drag measurements were made could differ from that of the aircraft due to the three-dimensional flow around the wing.

On this aircraft, it was unavoidable that the wake survey probe was placed behind a region of the wing where ailerons were present. The aileron deflections were measured by means of a potentiometer mounted on the aileron control cable.

The altitude, airspeed, temperature, aircraft angle of attack, and aileron deflection were recorded manually from digital readouts during each wake survey measurement.

FLIGHT TEST PROCEDURES

The aircraft was flown in clear air to establish an uniced baseline in terms of wing section drag coefficient plotted against aircraft angle of attack. This uniced baseline was used as a basis for comparison between the iced versus uniced aircraft.

The general procedure during icing flights was (1) accrete ice while measuring the icing environment (2) exit the icing cloud and document the wing ice shape with stereophotography (3) measure the increase in wing section drag with the wake survey probe at several airspeeds and (4) take additional stereophotographs during clear air wake probe traverses to determine if sublimation or erosion had altered the ice shape.

Airframe ice was accreted at cruise flight conditions (approximately 250 km/hr (135 KTAS)). While in icing, a relatively constant cruise airspeed was maintained by slowly increasing power. Icing instrumentation continuously measured icing cloud parameters during the encounter. The pneumatic deicer boots on the wings were not activated during the encounter allowing ice to build up on the wings. After a sufficient amount of ice had been accreted, the aircraft was flown out of the icing cloud. Generally the quickest means was to climb above the icing cloud.

At this point the stereo photographs and wake survey measurements were taken. During wake survey runs the airplane was flown steady and level with constant airspeed and angle of attack. About three to six measurements were usually taken, each at a specified airspeed. Stereo photographs were taken for each wake probe measurement.

During wake survey runs, no aileron inputs were intentionally made. The ailerons were left in a trim position and the rudder was used if necessary to maintain zero degree bank angle. However, the aileron trim position varied with airspeed. There was slightly more deflection at the lower airspeeds. (See table II). Positive deflections are down.

DATA REDUCTION

The icing instrumentation data was recorded on digital tape. After the flight the tape was read by an IBM 370 computer program which performed necessary calculations and then plotted the data in corrected engineering units for the desired time periods.

The analysis for the stereo photographs was performed by the Air Force's Arnold Engineering and Development Center. From the stereo photographs, the x-y-z coordinates of a definitive number of ice surface points were determined along a roughly 0.6 m (2 ft) spanwise section of the wing. The coordinates were then projected onto a single chordwise plane. Thus the ice accretion profile generated was a "composite" plot (figs. 15, 24, and 33). The scatter of the plotted points was indicative of each accretions roughness and spanwise variability. Reference 11 describes the equipment and data reduction methods in more detail.

The wake survey probe data analysis was done on an IBM 370. First the analog plot tracings from the flight tests were digitized and then a program was used to reduce the digitized data sets. The program did the following: converted raw data to engineering units; applied transducer calibrations; subtracted reference pressures from the pressure transducer outputs; applied nose-boom static pressure position error corrections; calculated vertical positions of the total and static pressure probes; interpolated the static pressure data in the wake to get static pressures that corresponded to total pressure measurements; allowed the user to determine limits of integration; and finally integrated the Jones equation (ref. 2) to determine wing section drag coefficient.

Figures 4 and 5 show typical variations of measured dynamic pressure and static pressure across the wake. Note that the static pressure varied considerably across the wake because the probes were located close to the wing trailing edge (1/4 chord). The wing has a chord of 1.981 m (6.5 ft) and a max thickness which is 16 percent of the chord. The "zero" probe arm position was defined as when the probe arm was parallel to the wing trailing edge. In this position the probe tips were about 14 cm (5.5 in.) above the wing chord.

RESULTS

Baseline (No Ice) Measurements

An uniced baseline was established as a basis for comparison between iced versus uniced cases. The baseline consisted of the wing section drag coefficient plotted against the aircraft angle of attack. This baseline is presented in figure 6 and represents data from two flights in clear air. The drag coefficient is plotted against angle of attack rather than lift coefficient because (1) the wing section lift coefficient was not measured during icing encounters and (2) the overall aircraft lift coefficient was altered by the presence of ice accretions on the wing.

The wake survey probe was also run prior to this season and initial data was published in reference 8. The data acquisition systems, transducers, and data reduction programs were entirely different for the two seasons. The earlier season employed a computerized data acquisition system that was not available for the 1984/85 icing season. The baseline shown in reference 8 does not fall on the baseline shown in figure 6. The reason for the discrepancy is not completely known, however two reasons justify the publication of the new data. The first reason is that the new data agrees better with numerical predictions from the Eppler airfoil analysis code (refs. 12 and 13). (See fig. 7). The second reason is that the primary interest is in the relative effects of the ice on the drag rather than the absolute numbers.

Also found in reference 8 is flight test data showing the uniced wing section lift coefficient as a function of aircraft angle of attack. This data was acquired by wrapping a pressure belt around the wing and measuring surface static pressures.

Icing Flight Measurements

Results are reported for three natural icing encounters for which there were adequate icing conditions and during which research instrumentation operated correctly, providing complete data sets. Data from each icing encounter is presented separately. For each encounter the order of discussion is as follows: (1) the icing environment and flight conditions (2) the resulting ice accretion on the wing and (3) the resulting drag increase caused by the ice. Table I summarizes the icing cloud conditions for each flight and table II summarizes the test conditions for the individual wake survey measurements.

Flight 85-17

The icing conditions encountered on flight 85-17 caused an accretion which was rime ice with a trough down the stagnation line. The average cloud liquid water content was 0.22 g/m^3. Because of this low LWC the aircraft flew in these conditions for 65 min before exiting the cloud. Figure 8 shows the large variability of the liquid water content during the encounter. The variability is interesting considering the fact that most icing simulations, whether in the wind tunnel or on a computer, generally assume constant LWC for practical reasons. The average droplet median volume diameter was 12.4 μm. The MVD varied little during the encounter compared to the LWC (see fig. 9). The average static air temperature was -11.5 °C and was relatively constant

(fig. 10). The average true airspeed was 215 km/hr (116 kts) and varied as shown in figure 11. The average altitude was 1254 m (4114 ft). Note on figure 12 that the aircraft descended into the icing cloud at the beginning and then descended out of the cloud at the end when enough ice had been accreted. Figure 13 shows the aircraft angle of attack during the encounter.

Figure 14 presents a photograph of the ice accretion on the wing. This portion of the wing was directly ahead of the area where wake survey measurements were made. The photographs were originally color and were reprinted in black and white. Some of the detail is therefore lost. Note that the solid white color is characteristic of rime ice while the trough along the leading edge is a glaze characteristic.

Figure 15 shows a cross sectional profile of the ice accretion on the leading edge of the wing which was generated from the stereophotography analysis. As mentioned previously these data points represent locations of the ice surface measured anywhere along a 0.6 m (2 ft) spanwise section. Thus the profile is a composite ice shape representing both the general shape and the variability of the ice surface at different locations. The stereo profile is most useful for quantifying the general size of the accretion.

Figure 16 presents the increase in wing section drag coefficient due to the ice accretion. Wake Survey probe measurements from the icing flight are compared to the uniced baseline. For the same aircraft angle of attack of 2°, the iced drag coefficient shows an increase over the baseline of 15 percent. A line was fit through these data using the method of least squares. Curve fit results are presented in table III.

Flight 85-24a

Flight 85-24a was an encounter with mixed icing (i.e., mix between rime and glaze icing). The average LWC was 0.45 g/m^3 (fig. 17). The average MVD was 19.5 μm. Note on figure 18 that the FSSP laser probe was not working during part of the icing encounter. The laser probe iced up during the first two thirds of the encounter. The assumption is made that the MVD was the same during the entire encounter since MVD's have been observed to be relatively constant in stratiform clouds. Also the assumption is made that the laser probe was working correctly when it was not iced up. It is assumed that it was not partially blocked by ice. From past experience laser probe icing seems to cause total failure of the probe rather than produce merely erroneous results. The exception to this is when large quantities of ice accrete on the laser pod shell and actually change the aerodynamic flow around the probe. The amount of ice on the probe shell can be seen from the aircraft cabin and was judged to be acceptable in this case. Considering the assumptions that had to be made, the MVD measurement for flight 85-24a was the most uncertain of the three flights.

The average static air temperature was -14.8 °C (fig. 19). The average true airspeed was 257 km/hr (139 kts) (fig. 20). The average pressure altitude was 2008 m (6588 ft) (fig. 21). The average aircraft angle of attack was 0.9° (fig. 22).

Figure 23 shows a photograph of the ice accretion on the wing. The ice is nearly clear in the center which is a glaze characteristic. Along the edges

of the accretion the ice is more like rime. One might wonder why flight 85-17 was rime ice and flight 85-24a was mixed ice when the temperature was colder on flight 85-24a. The reasons are that flight 85-17 had a much lower LWC and smaller droplet sizes so the freezing fraction was greater. Figure 24 presents the profile generated from the stereo photographs.

Figure 25 shows the increase in wing section drag coefficient due to the ice accretion. At an aircraft angle of attack of 2°, the drag coefficient increased 23 percent over the baseline. Six measurements were taken with ice on the wing. It is believed that measurements 4 to 6 are lower than they should be due to ice erosion and sublimation; therefore they were not included in the figure. The change in the ice shape was caused by the fact that after sufficient ice had accreted on the aircraft it was flown out of the clouds, into the sun, to terminate icing. The sunlight hastened the sublimation of the ice even though the temperature was still cold. The general procedure was to fly away from the sun, (when possible) in an attempt to shield the ice accretion from the sun for as long as possible. Also to minimize sublimation, measurements were begun with the low speed data points first and then followed with the higher speed data points.

Flight 85-24b

Flight 85-24b was another mixed icing encounter. The aircraft was in icing conditions for 20 min. The average LWC was 0.46 g/m^3 (fig. 26). The average MVD was 15.1 μm (fig. 27). Note that the laser probe iced over towards the end of the encounter when the LWC and icing rate were very high. The average static air temperature was -14.3 °C (fig. 28). The average true airspeed was 259 km/hr (140 kts) (fig. 29). The variations in airspeed were caused by turbulence in the icing cloud. Also, the pilot sometimes changed altitude slightly to stay in the best icing conditions. The average altitude was 1976 m (6483 ft) (fig. 30). The average aircraft angle of attack was 1.2° (fig. 31).

A photograph of the ice accretion on the wing is shown in figure 32. The corresponding profile generated from stereophotography analysis is shown in figure 33. The accretion is very similar to that of Flight 85-24a since the environment was nearly the same, but this accretion is slightly larger; with small "horns" that were probably caused by the additional five minutes in icing conditions.

The resulting increase in wing section drag coefficient over the uniced baseline is presented in figure 34. Due to the larger ice accretion, the drag increase is greater for this case. At a 2° angle of attack, the drag increase was 39 percent of the uniced baseline.

CONCLUSIONS

Three data sets have been collected which can be used to begin comparisons between natural icing in flight and simulated icing; either in an icing research tunnel or using computer codes. Flight 85-24b is the best data set for comparison purposes because the largest ice accretion and the largest drag increase were observed on that flight. Flight 85-24a was very similar to

85-24b except the ice accretion was slightly smaller and the drag rise less. Flight 85-24a had the most uncertain MVD measurement of the three encounters.

Flight 85-17 had the most data points associated with the drag plot but unfortunately the drag rise was rather small. Also the LWC was very low (0.22 g/m^3), and the icing duration was very long (65 min) making the encounter difficult to simulate.

All three flights had highly variable LWC's during the encounter. This variability could be compared to the constant icing conditions which are produced in an icing wind tunnel. All three flights had similar ice shapes which are a mix between rime and glaze ice. This is primarily due to the temperatures being relatively close. It would be highly desirable to document additional encounters which produce more pure rime and glaze ice accretions (i.e., ice formed at very cold temperatures and at temperatures very near freezing, respectively). Also, flights are desired where the accretions are large. A larger ice accretion takes on a more unique shape which is a function of the physics involved. These larger shapes are then a more significant test when comparing flight results to simulated icing results, either in the wind tunnel or on the computer.

REFERENCES

1. Jones, B.M.: Measurement of Profile Drag by the Pitot Traverse Method. R.&M. No. 1688, British A.R.C., 1936.

2. Gregorek, G.M., et al.: Inflight Measurements of the GA(W)-2 Aerodynamic Characteristics. SAE Paper 770461, Mar. 1977.

3. Shaw, R.J.; Sotos, R.G.; and Solano, F.R.: An Experimental Study of Airfoil Icing Characteristics. AIAA Paper 82-0283, Jan. 1982.

4. Olsen, W.; Shaw, R.; and Newton, J.: Ice Shapes and the Resulting Drag Increase for a NACA 0012 Airfoil. AIAA Paper 84-0109, Jan. 1984.

5. Olsen, W.; Takeuchi, D.; and Adams, K.: Experimental Comparison of Icing Cloud Instruments. AIAA Paper 83-0026, Jan. 1983.

6. Ide, R.F.; and Richter, G.P.: Comparison of Icing Cloud Instruments for 1982-83 Icing Season Flight Program. AIAA Paper 84-0020, Jan. 1984.

7. Ranaudo, R.J., et al.: Performance Degradation of a Typical Twin Engine Commuter Type Aircraft in Measured Natural Icing Conditions. AIAA Paper 84-0179, Jan. 1984.

8. Mikkelsen, K.L., et al.: Icing Flight Research: Aerodynamic Effects of Ice and Ice Shape Documentation with Stereo Photography. AIAA Paper 85-0468, Jan. 1985.

9. Shaw, R.J.: Progress Toward the Development of an Aircraft Icing Analysis Capability. AIAA Paper 84-0105, Jan. 1984.

10. Taylor, J.R.W., ed.: Jane's All the Worlds Aircraft, Franklin Watts Inc., 1978.

11. McKnight, R.C.; Palko, R.L.; and Humes, R.L.: In-flight Photogrammetric Measurement of Wing Ice Accretions. AIAA Paper 86-0483, Jan. 1986.

12. Numerical predictions were provided by Dr. Robert J. Shaw, NASA Lewis Research Center.

13. Eppler, R.; and Somers, D.M.: A Computer Program for the Design and Analysis of Low-Speed Airfoils. NASA TM-80210, 1980.

TABLE I. - SUMMARY OF ICING CLOUD CONDITIONS

Flight data	Flight number		
	85-17	85-24a	85-24b
	Date		
	3/15/85	4/2/85	4/2/85
1. Average pressure altitude, m	1254	2008	1976
2. Average true airspeed, km/hr	215	257	259
3. Average aircraft angle of attack, deg	2.4	0.9	1.2
4. Average right aileron deflection, deg	-1.2	-1.1	-0.9
5. Start time of icing encounter	09:48	09:55	10:49
Icing cloud data			
6. Average static temperature, °C	-11.5	-14.8	-14.3
7. Average cloud liquid water content, g/m^3	0.22	0.45	0.46
8. Average median volume droplet diameter, μm	12.4	19.5	15.1
9. Duration of encounter, min	65	15	20
10. Extent of encounter, km	233	64	86
Ice accretion properties			
11. Type of ice	Rime	Mixed	Mixed
12. Shape of ice (see photo and profile)			

TABLE II. - TEST CONDITIONS AND WING SECTION DRAG DATA

Flight	Run	True airspeed, km/hr	Mach number	Reynolds number	Aircraft angle of attack, α, deg	Aileron deflection, deg	Wing C_d
No ice on wing							
85-12	1	294	0.246	9.85×10^6	-0.2	-1.0	0.0112
	2	249	.208	8.29	1.1	-.9	.0123
	3	216	.181	7.16	2.7	-1.4	.0130
	4	189	.158	6.26	4.6	-1.7	.0147
	5	171	.143	5.71	6.3	-1.7	.0156
	6	153	.128	5.15	8.8	-1.9	.0175
	7	294	.245	9.81	-.4	-1.0	.0111
	8	247	.206	8.24	1.1	-1.1	.0127
	9	213	.178	7.15	2.7	-1.5	.0119
	10	186	.156	6.21	4.6	-1.6	.0132
	11	167	.139	5.57	6.6	-2.1	.0138
	12	154	.129	5.16	9.2	-2.3	.0166
	13	249	.208	8.33	.7	-1.2	.0104
85-21	1	278	0.234	9.81×10^6	-0.1	-0.9	0.0118
	2	239	.202	8.41	1.4	-.9	.0129
	3	212	.179	7.44	2.5	-.9	.0140
	4	194	.164	6.84	3.9	-1.0	.0142
	5	170	.144	5.99	5.6	-.8	.0156
	6	158	.133	5.57	7.1	-.9	.0164
	7	148	.125	5.21	8.5	-.6	.0177
	8	142	.12	4.98	11.3	-.8	.0185
	9	142	.12	4.99	11.3	-.6	.0190
Ice on wing							
85-17	1	155	0.133	6.2×10^6	7.8	-1.1	0.0201
	2	177	.151	6.38	4.9	-1.1	.0173
	3	204	.175	7.38	2.8	-.9	.0149
	4	274	.234	9.87	-.1	-.7	.0131
	5	160	.137	5.71	7.8	-.9	.0210
85-24a	1	180	0.155	6.03×10^6	6.3	-1.4	0.0200
	2	218	.188	7.23	2.9	-.8	.0159
	3	272	.234	9.13	.3	-.7	.0142
	4	271	.234	9.00	.5	-.7	.0133
	5	221	.190	7.37	2.7	-1.0	.0139
	6	192	.165	6.42	4.9	-1.1	.0168
85-24b	1	178	0.153	5.97×10^6	6.2	-1.4	0.0219
	2	216	.186	7.24	2.6	-1.1	.0187
	3	273	.235	9.15	.5	-.8	.0157

TABLE III. - CURVE FITS OF DRAG DATA
(LEAST SQUARES METHOD)

Clean wing	$C_d = 0.0114 + 0.00065\ \alpha$
Ice flight 85-17	$C_d = 0.0127 + 0.00098\ \alpha$
Ice flight 85-24a	$C_d = 0.0136 + 0.00098\ \alpha$
Ice flight 85-24b	$C_d = 0.0155 + 0.00107\ \alpha$

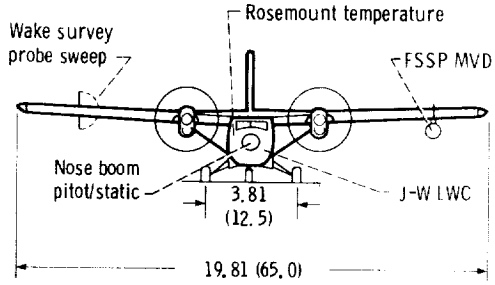

Figure 1. - Research probe locations. (Dimensions are in meters (feet).)

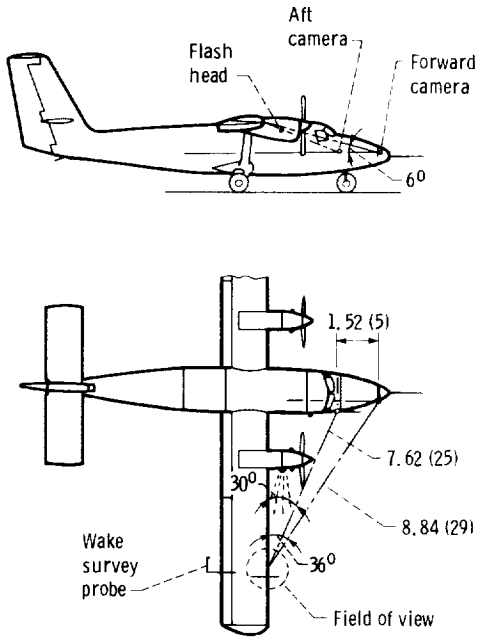

Figure 2. - Layout of stereo camera system. (Dimensions are in meters (feet).)

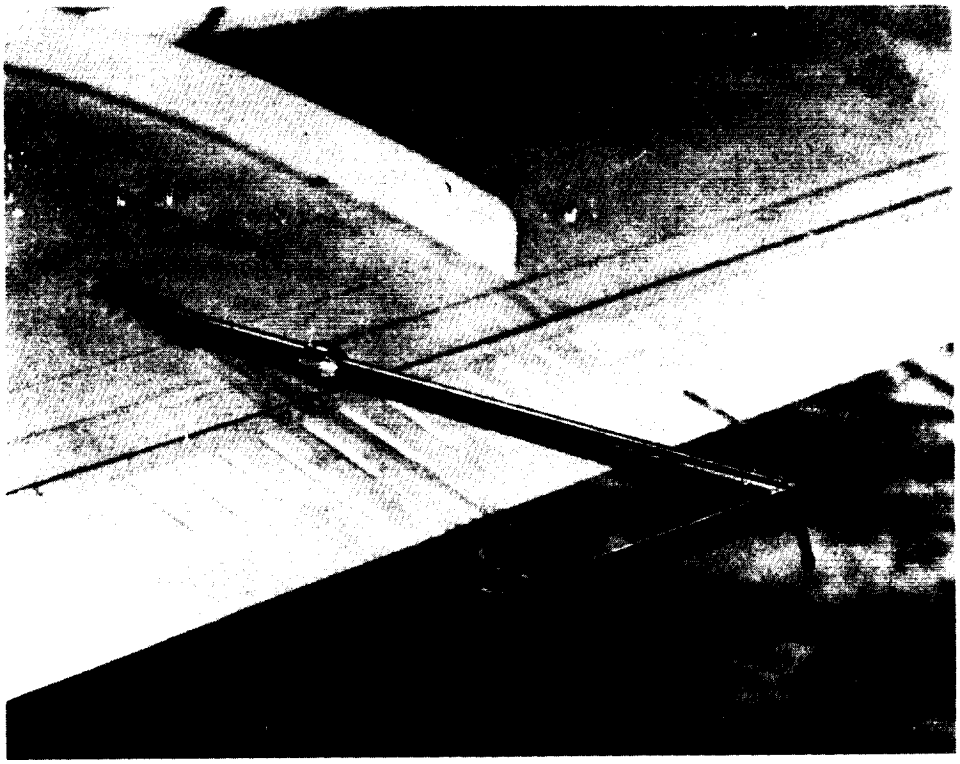

Figure 3. - Wake survey probe on right wing.

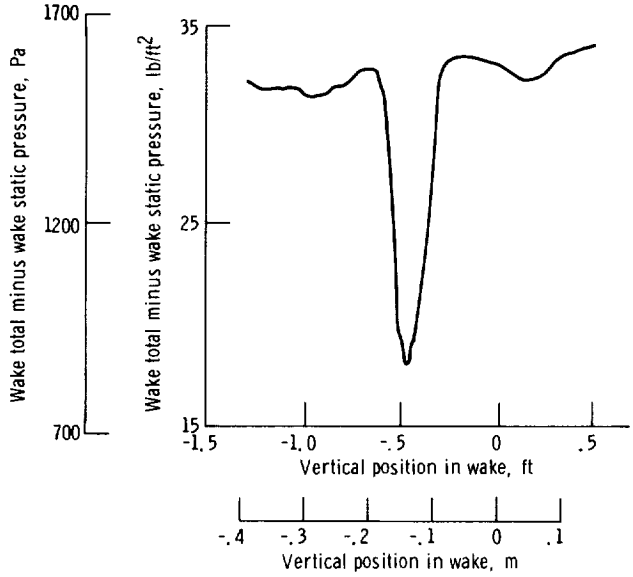

Figure 4. - Typical variation of dynamic pressure across wing wake - flight 85-12, run 9.

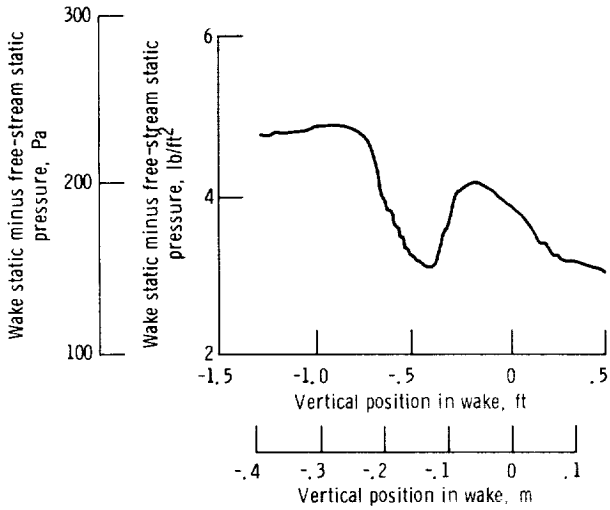

Figure 5. - Typical variation of static pressure across wing wake - flight 85-12, run 9.

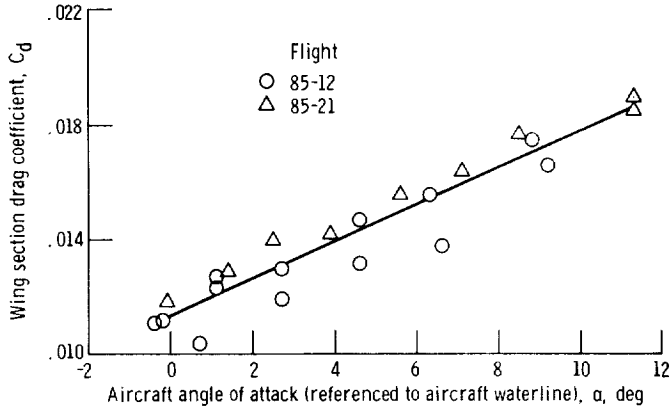

Figure 6. - Variation in wing section drag coefficient with aircraft angle of attack for wing with no ice.

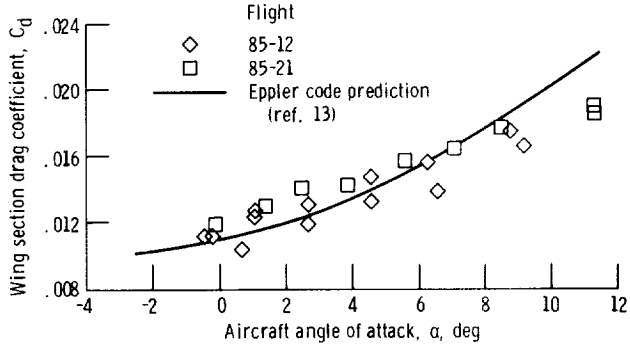

Figure 7. - Comparison of flight test baseline results with numerical prediction (for wing with no ice). (Prediction assumes that wing angle of attack equals aircraft angle of attack plus 2.5^0.)

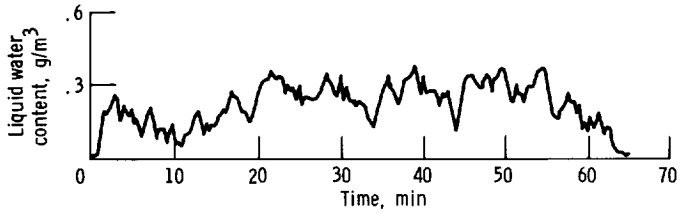

Figure 8. - Variation in cloud liquid water content during icing encounter - flight 85-17.

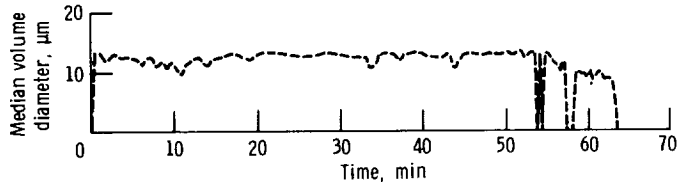

Figure 9. - Cloud median volume droplet diameter during icing encounter - flight 85-17.

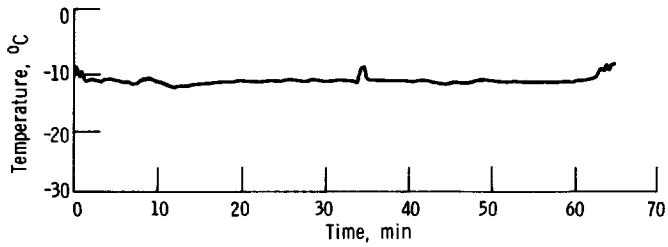

Figure 10. - Static air temperature during icing encounter - flight 85-17.

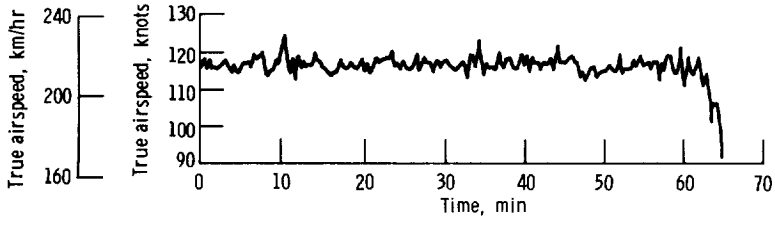

Figure 11. - True airspeed during icing encounter - flight 85-17.

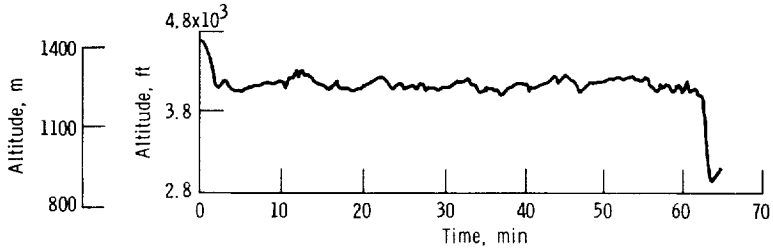

Figure 12. - Pressure altitude during icing encounter - flight 85-17.

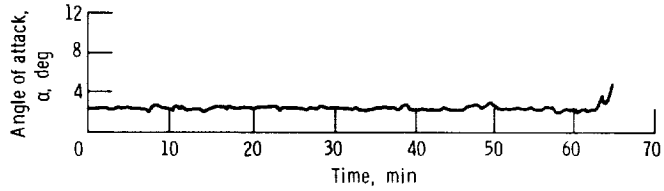

Figure 13. - Aircraft angle of attack (referenced to aircraft waterline) during icing encounter - flight 85-17.

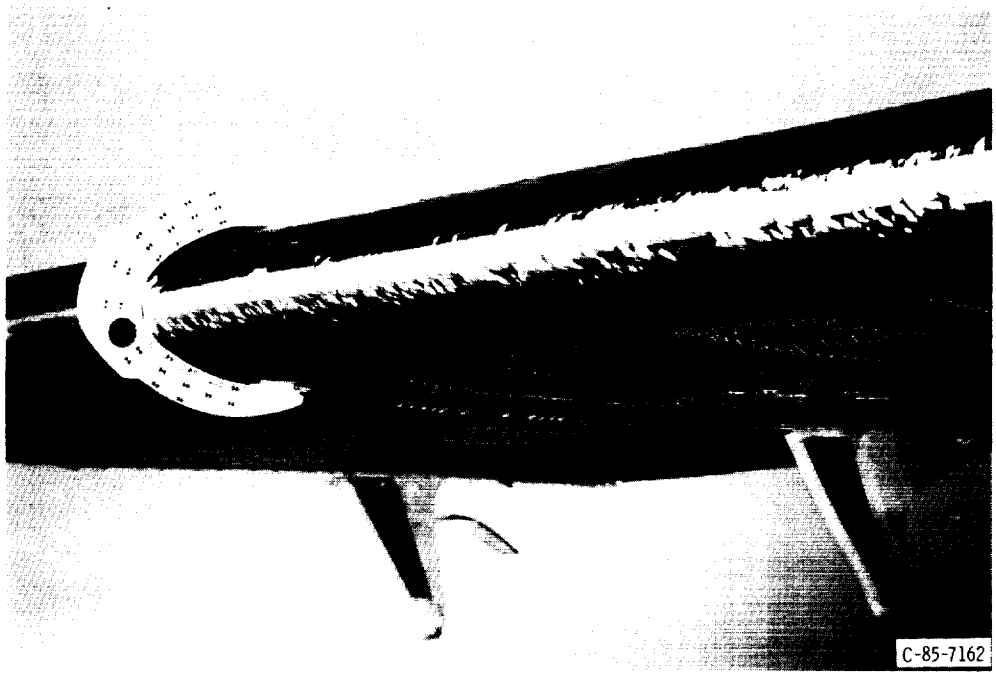

Figure 14. - Ice accretion on wing - flight 85-17.

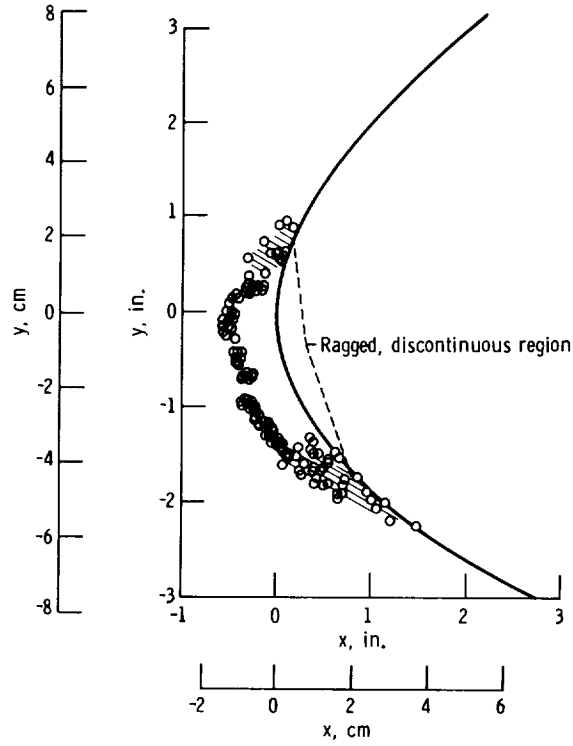

Figure 15. - Ice accretion profile generated from stereo photography - flight 85-17.

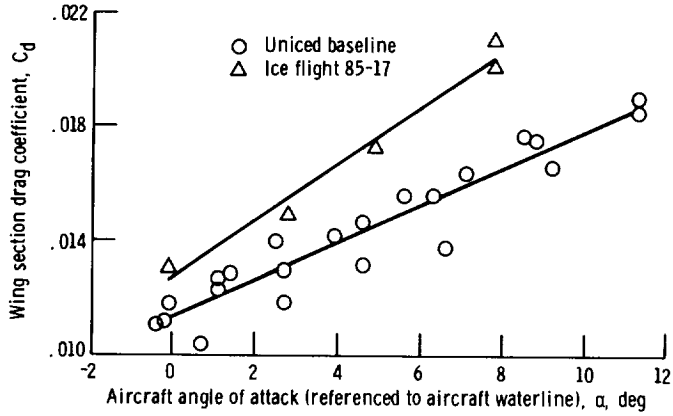

Figure 16. - Increase in wing section drag coefficient due to rime ice - flight 85-17.

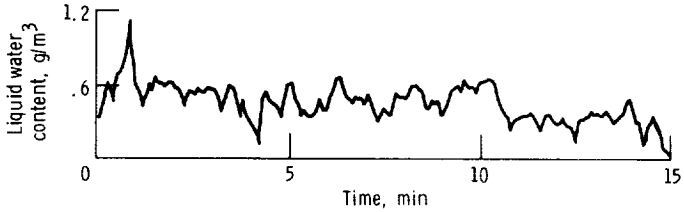

Figure 17. - Variation in cloud liquid water content during icing encounter - flight 85-24a.

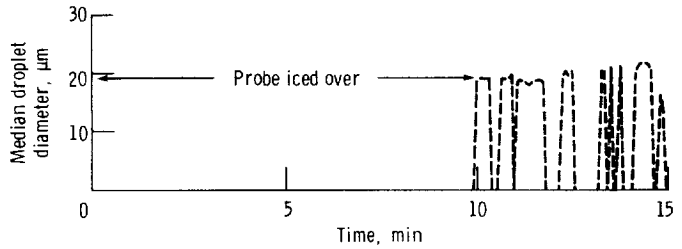

Figure 18. - Cloud median volume droplet diameter during icing encounter - flight 85-24a. (Probe iced over during part of encounter.)

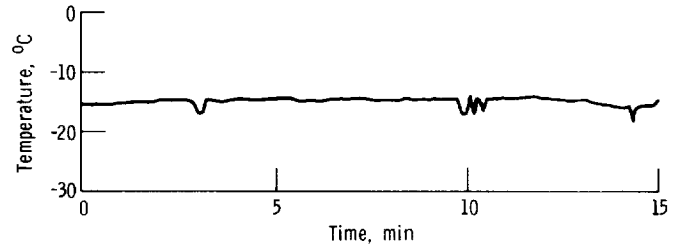

Figure 19. - Static air temperature during icing encounter - flight 85-24a.

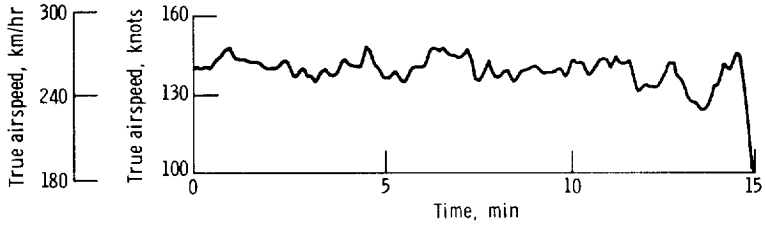

Figure 20. - Aircraft true airspeed during icing encounter - flight 85-24a.

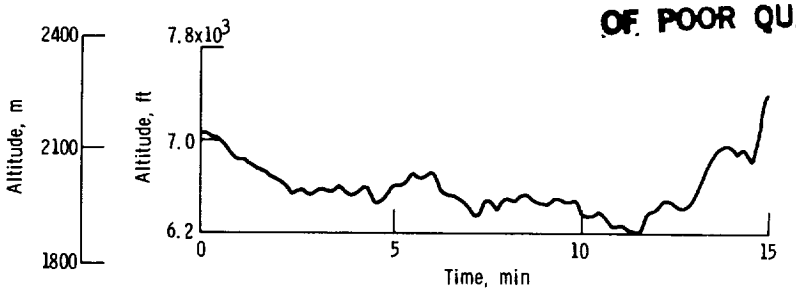

Figure 21. - Aircraft pressure altitude during icing encounter - flight 85-24a.

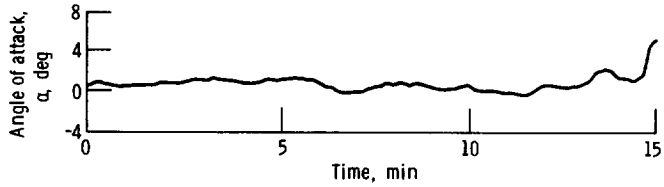

Figure 22. - Aircraft angle of attack (referenced to aircraft waterline) during icing encounter - flight 85-24a.

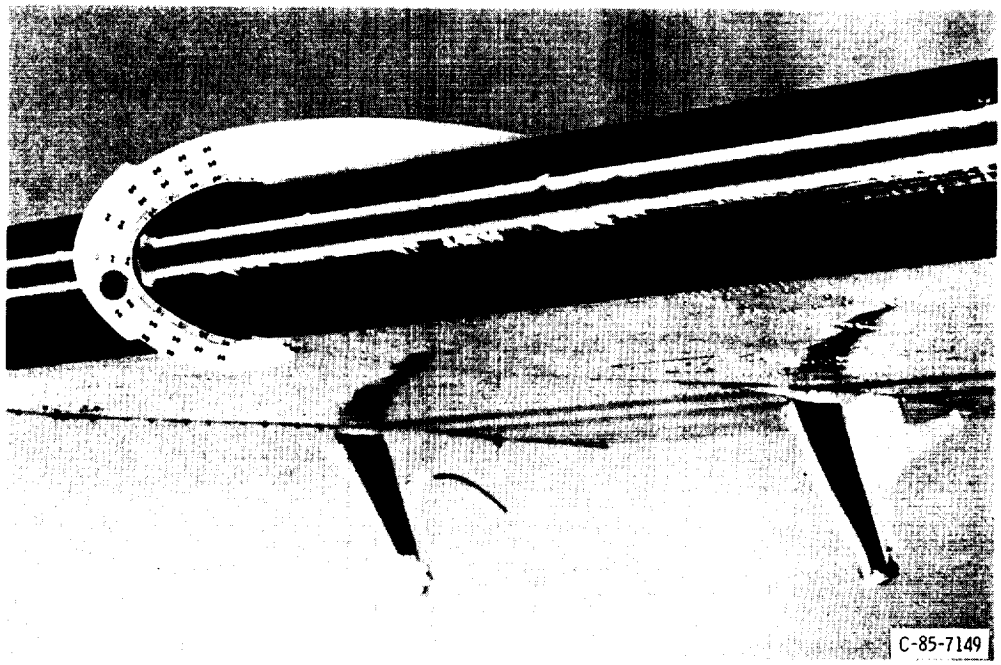

Figure 23. - Ice accretion on wing - flight 85-24a.

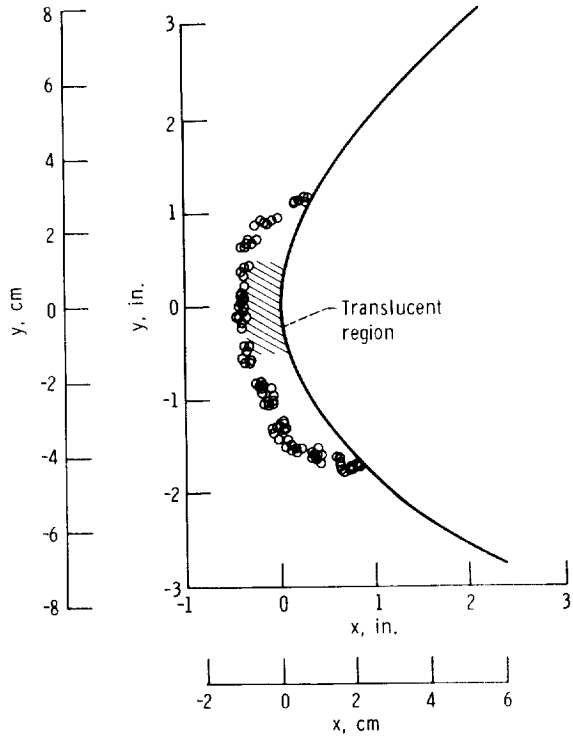

Figure 24. - Ice accretion profile generated from stereo photography - flight 85-24a.

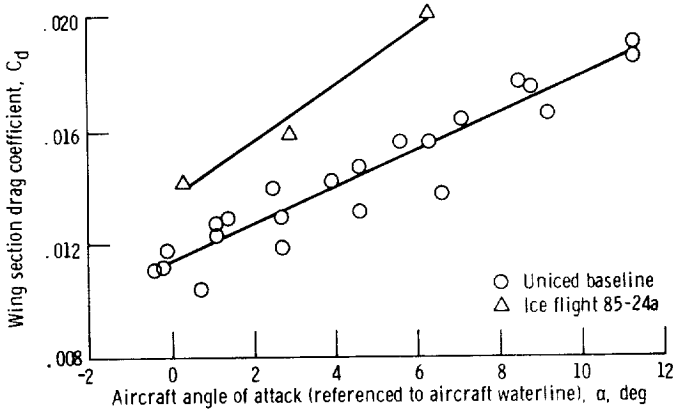

Figure 25. - Increase in wing section drag coefficient due to mixed ice - flight 85-24a.

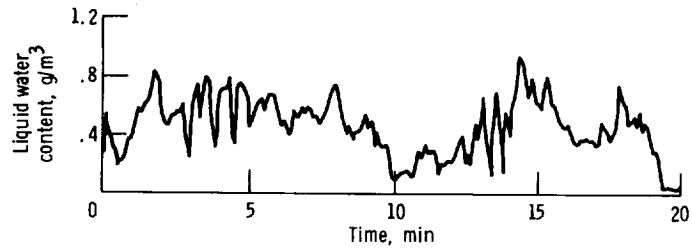

Figure 26. - Variation in cloud liquid water content during icing encounter - flight 85-24b.

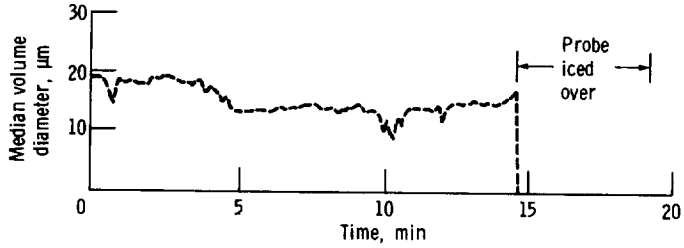

Figure 27. - Cloud median volume droplet diameter during icing encounter - flight 85-24b.

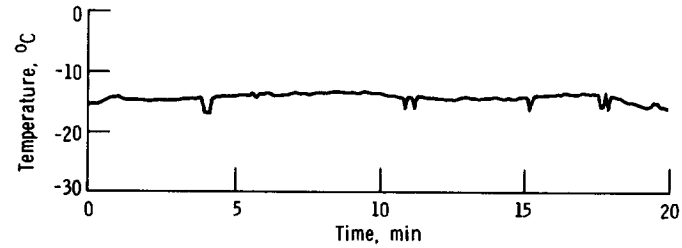

Figure 28. - Static air temperature during icing encounter - flight 85-24b.

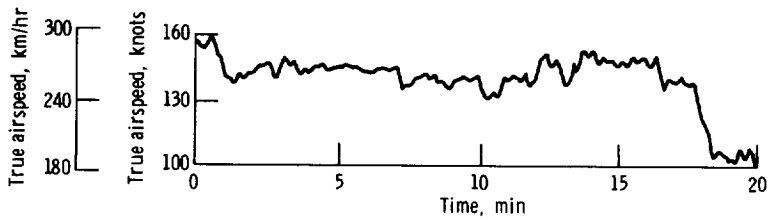

Figure 29. - Aircraft true airspeed during icing encounter - flight 85-24b.

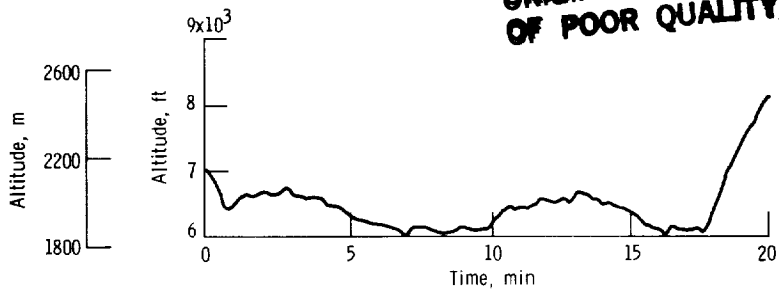

Figure 30. - Aircraft pressure altitude during icing encounter - flight 85-24b.

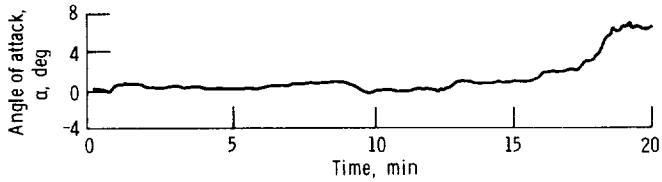

Figure 31. - Aircraft angle of attack (referenced to aircraft waterline) during icing encounter - flight 85-24b.

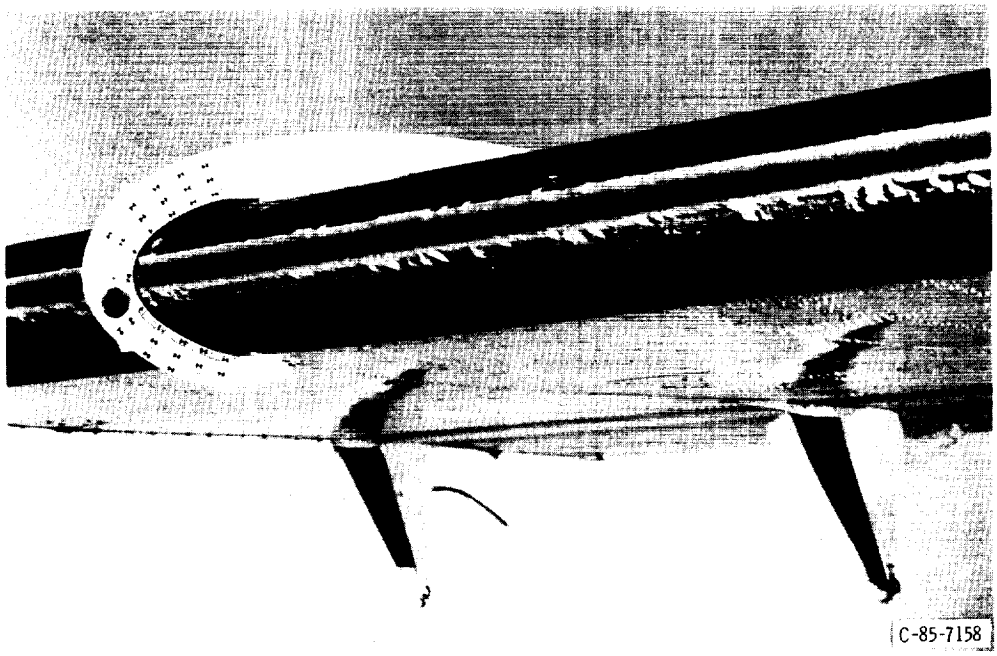

Figure 32. - Ice accretion on wing - flight 85-24b.

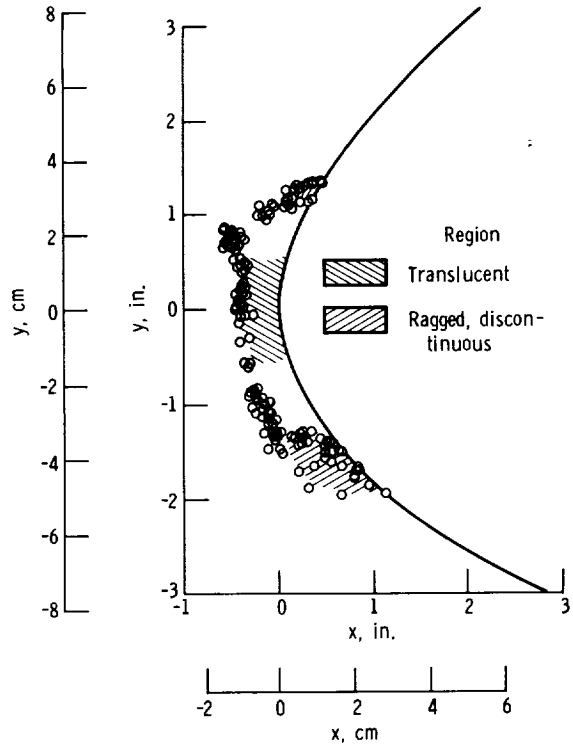

Figure 33. - Ice accretion profile generated from stereo photography - flight 85-24b.

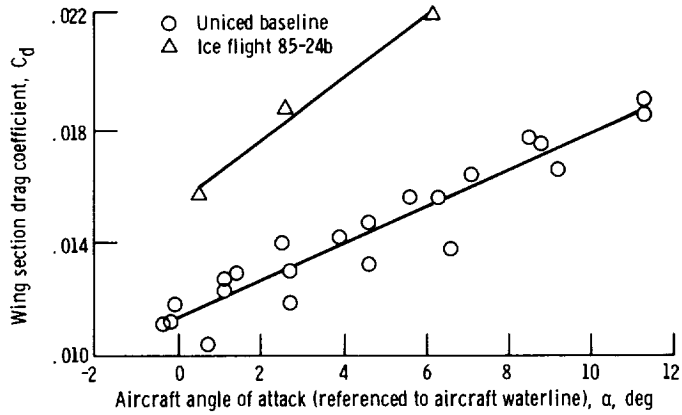

Figure 34. - Increase in wing section drag coefficient due to mixed ice - flight 85-24b.

1. Report No.	2. Government Accession No.	3. Recipient's Catalog No.
NASA TM-87301		

4. Title and Subtitle	5. Report Date
In-Flight Measurements of Wing Ice Shapes and Wing Section Drag Increases Caused by Natural Icing Conditions	April 1986
	6. Performing Organization Code: 505-68-11

7. Author(s)	8. Performing Organization Report No.
Kevin Mikkelsen, Nikola Juhasz, Richard Ranaudo, Robert McKnight, Robert Freedman, and John Greissing	E-3013
	10. Work Unit No.

9. Performing Organization Name and Address	11. Contract or Grant No.
National Aeronautics and Space Administration Lewis Research Center Cleveland, Ohio 44135	
	13. Type of Report and Period Covered: Technical Memorandum

12. Sponsoring Agency Name and Address	14. Sponsoring Agency Code
National Aeronautics and Space Administration Washington, D.C. 20546	

15. Supplementary Notes

16. Abstract

Aircraft icing flight research was performed in natural icing conditions with a twin engine commuter type STOL aircraft. In-flight measurements were made of the icing cloud environment, the shape of the ice accretion on the wing, and the corresponding increase in the wing section drag. Results are presented for three icing encounters. On one flight, the wing section drag coefficient increased 35 percent over the uniced baseline for cruise conditions while a 43 percent increase was observed at an angle of attack of 6.2°.

17. Key Words (Suggested by Author(s))	18. Distribution Statement
Wing icing Icing research	Unclassified - unlimited STAR Category 02

19. Security Classif. (of this report)	20. Security Classif. (of this page)	21. No. of pages	22. Price*
Unclassified	Unclassified		

*For sale by the National Technical Information Service, Springfield, Virginia 22161